

# Phase diagrams in the Hadron-PNJL model

G.Y. Shao,<sup>1</sup> M. Di Toro,<sup>1,2,\*</sup> V. Greco,<sup>1,2</sup> M. Colonna,<sup>1</sup> S. Plumari,<sup>1,2</sup> B. Liu,<sup>3,4</sup> and Y.X. Liu<sup>5,6</sup>

<sup>1</sup>*INFN-Laboratori Nazionali del Sud, Via S. Sofia 62, I-95123 Catania, Italy*

<sup>2</sup>*Physics and Astronomy Dept., University of Catania, Italy*

<sup>3</sup>*IHEP, Chinese Academy of Sciences, Beijing, 100049 China*

<sup>4</sup>*Theoretical Physics Center for Scientific Facilities,  
Chinese Academy of Sciences, Beijing, 100049 China*

<sup>5</sup>*Department of Physics and State Key Laboratory of  
Nuclear Physics and Technology, Peking University, Beijing 100871, China*

<sup>6</sup>*Center of Theoretical Nuclear Physics,  
National Laboratory of Heavy Ion Accelerator, Lanzhou 730000, China*

The two-Equation of State (Two-EoS) model is used to describe the hadron-quark phase transition in dense-hot matter formed in heavy-ion collisions. The non-linear Walecka model is used to describe the hadronic phase. For the quark phase, the Nambu–Jona-Lasinio model coupled to Polyakov-Loop fields (PNJL) is used to include both the chiral and (de)confinement dynamics. The phase diagrams are derived from the Gibbs conditions and compared with the results obtained in the Hadron-NJL model without confinement. As in the Hadron-NJL case a first order transition is observed, but with a Critical-End-Point at much higher temperature, consequence of the confinement mechanism that reduces the degrees of freedom of the quark matter in proximity of the phase transition. Particular attention is devoted to the phase transition in isospin asymmetric matter. Interesting isospin effects are found at high baryon density and reduced temperatures, in fact common also to other quark models, like MIT-Bag and NJL model. Some possible observation signals are suggested to probe in Heavy-Ion Collision (HIC) experiments at intermediate energies.

PACS numbers: 12.38.Mh, 25.75.Nq

## I. INTRODUCTION

The exploration of the phase diagram of strongly interacting matter and search for the signals of the phase transition from hadronic to quark-gluon phase are very important in both theory and experiment. As a fundamental tool, lattice QCD provides us the best framework for investigation of non-perturbative phenomena such as confinement and quark-gluon plasma formation at finite temperature and vanishing (small) chemical potential [1–7]. However, lattice QCD suffers the serious problem of the fermion determinant with three color at finite  $\mu$ . Although several approximation methods have been taken to try to evade this problem [8–12], the validity of lattice simulations at finite chemical potential is still limited to the region  $\mu_q/T < 1$  [13]. The results obtained with  $\mu_q/T > 1$  should be taken with care.

On the other hand, many phenomenological models [14–17], as well as the more microscopic Dyson-Schwinger equations (DSEs) approach [18], have been proposed to derive a complete description of QCD phase diagram. Among these effective models, the Nambu–Jona-Lasinio model (NJL) is a predominant one, since it offers a simple illustration of chiral symmetry breaking and restoration, a key feature of QCD [19–25]. Moreover, it provides a complicated phase diagram of color superconductivity at high density [26–28]. One deficiency of the standard

NJL model is that quarks are not confined. Recently, an improved version of the NJL model coupled to Polyakov-Loop fields (PNJL) has been proposed [29]. The PNJL model takes into account both the chiral symmetry and (de)confinement effect, giving a good interpretation of lattice data at zero chemical potential and finite temperature. At the same time it is able to make predictions in regions that cannot be presently reached in lattice calculation [30–36].

Most effective models, including the PNJL model, describe the hadron–quark-gluon phase transition based on quark degrees of freedom. As a matter of fact, at low temperature and small chemical potential, QCD dynamics should be governed by hadrons. Therefore, it is natural to describe the strongly interacting matter with hadronic degrees of freedom at low  $T$  and small  $\mu$  and quarks at high  $T$  and large  $\mu$ . This picture can be easily realized following a two equation of state (Two-EoS) model, where hadronic and quark phases are connected by the Gibbs (Maxwell) criteria. Such approach is widely used in describing the phase transition in the interior of compact star in beta-equilibrium (e.g., [37–43]). Recently, it has also been adopted to explore the phase diagram of hadron-quark transition at finite temperature and density related to Heavy-Ion Collision (HIC) [44, 46–49]. Moreover, in these studies more attention was paid to isospin asymmetric matter, and some observable effects have been suggested to be seen in charged meson yield ratio and on the onset of quark number scaling of the meson/baryon elliptic flows in Ref. [46, 47]. Such heavy ion connection provides us a new orientation to investigate the hadron-quark phase transition, and it can stimulate

---

\*Corresponding author: [ditoro@lns.infn.it](mailto:ditoro@lns.infn.it)

some new relevant researches in this field.

We have previously studied the hadron-quark phase transition in the Two-EoS model by using the MIT-Bag model [47] and NJL model [50] to describe quark matter, respectively. In particular a kind of Critical-End-Point (CEP) of a first order transition has been found at about  $T = 80$  MeV and  $\mu = 900$  MeV when NJL model is considered for the quark matter. In this paper, in order to obtain more reliable results and predict possible observables in the experiments, an improved calculation, within the Two-EoS approach, has been performed. We take the PNJL Lagrangian to describe the properties of quark matter, with the interaction between quarks and Polyakov-Loop, where both the chiral and (de)confinement dynamics are included simultaneously. We are not considering here color pairing correlations, that are affecting the isospin asymmetry [49], since in heavy ion collisions the high density system will be always formed at rather large temperatures [46].

We obtain the phase diagrams of hadron-quark-gluon phase transition in  $T - \rho_B$  and  $T - \mu_B$  planes. We compare the obtained results with those given in [50] where the NJL model is used to describe the quark phase. The calculation shows that the phase-transition curves are greatly modified when both the chiral dynamics and (de)confinement effect are considered, in particular in the high temperature and low chemical potential region. We still see a first order transition but the CEP is now at much higher temperature and lower chemical potential. In fact the CEP temperature is much closer to the critical temperature (for a crossover) given by lattice calculation at vanishing chemical potential. Our results seem to stress the importance of an extension of lattice calculations up to quark chemical potentials around  $\mu_q/T_c \simeq 1$ .

In addition we address the discussion about the non-coincidence of chiral and deconfinement phase transition at large chemical potential and low temperature, relevant to the formation of quarkonic matter.

Finally the calculation confirms that the onset density of hadron-quark phase transition is much smaller in isospin asymmetric than that of symmetric matter, and

therefore it will be more easy to probe the mixed phase in experiments.

The paper is organized as follows. In Section II, we describe briefly the Two-EoS approach and give the relevant formulae of the hadronic non-linear Walecka model and the PNJL effective theory. In Section III, we discuss the expected effects of the confinement dynamics. The quark matter phase transition are presented in Section IV for the NJL as well as the PNJL models. Section V is devoted to the phase diagrams within the Two-EoS frame to the comparison with the results using only the pure quark PNJL model to describe both phases. Moreover, we present some discussions and conclusions about the phase transition, as well as some suggestions for further study. Finally, a summary is given in Section VI.

## II. HADRON MATTER, QUARK MATTER AND THE MIXED PHASE

In our Two-EoS approach, the hadron matter and quark matter are described by the non-linear Walecka model and by the PNJL model, respectively. For the mixed phase between pure hadronic and quark matter, the two phases are connected each other with the Gibbs conditions deduced from thermal, chemical and mechanical equilibriums. In this section, we will first give a short introduction of the nonlinear Walecka model for the hadron matter and the PNJL model for quark matter, then we construct the mixed phase with the Gibbs criteria based on baryon and isospin charge conservations during the transition.

For hadron phase, the non-linear Relativistic Mean Field (RMF) approach is used, which provides an excellent description of nuclear matter and finite nuclei as well as of compressed matter properties probed with high energy HIC [44, 46, 47, 51, 52]. The exchanged mesons include the isoscalar-scalar meson  $\sigma$  and isoscalar-vector meson  $\omega$  ( $NL$  force, for isospin symmetric matter), isovector-vector meson  $\rho$  and isovector-scalar meson  $\delta$ , ( $NL\rho$  and  $NL\rho\delta$  forces, for isospin asymmetric matter).

The effective Lagrangian is written as

$$\begin{aligned} \mathcal{L} = & \bar{\psi}[i\gamma_\mu\partial^\mu - M + g_\sigma\sigma + g_\delta\boldsymbol{\tau} \cdot \boldsymbol{\delta} - g_\omega\gamma_\mu\omega^\mu - g_\rho\gamma_\mu\boldsymbol{\tau} \cdot \boldsymbol{\rho}^\mu]\psi \\ & + \frac{1}{2}(\partial_\mu\sigma\partial^\mu\sigma - m_\sigma^2\sigma^2) - \frac{1}{3}b(g_\sigma\sigma)^3 - \frac{1}{4}c(g_\sigma\sigma)^4 + \frac{1}{2}(\partial_\mu\delta\partial^\mu\delta - m_\delta^2\delta^2) \\ & + \frac{1}{2}m_\omega^2\omega_\mu\omega^\mu - \frac{1}{4}\omega_{\mu\nu}\omega^{\mu\nu} + \frac{1}{2}m_\rho^2\rho_\mu \cdot \rho^\mu - \frac{1}{4}\rho_{\mu\nu} \cdot \rho^{\mu\nu}, \end{aligned} \quad (1)$$

where the antisymmetric tensors of vector mesons are given by

$$\omega_{\mu\nu} = \partial_\mu\omega_\nu - \partial_\nu\omega_\mu, \quad \rho_{\mu\nu} \equiv \partial_\mu\rho_\nu - \partial_\nu\rho_\mu.$$

The nucleon chemical potential and effective mass in

nuclear medium can be expressed as

$$\mu_i = \mu_i^* + g_\omega\omega + g_\rho\tau_{3i}\rho, \quad (2)$$

and

$$M_i^* = M - g_\sigma\sigma - g_\delta\tau_{3i}\delta, \quad (3)$$

where  $M$  is the free nucleon mass,  $\tau_{3p} = 1$  for proton and  $\tau_{3n} = -1$  for neutron, and  $\mu_i^*$  is the effective chemical potential which reduces to Fermi energy  $E_{F_i}^* = \sqrt{k_F^2 + M_i^{*2}}$  at zero temperature. The baryon and isospin chemical potentials in the hadron phase are defined as

$$\mu_B^H = \frac{\mu_p + \mu_n}{2}, \quad \mu_3^H = \frac{\mu_p - \mu_n}{2}. \quad (4)$$

$$\varepsilon^H = \sum_{i=p,n} \frac{2}{(2\pi)^3} \int d^3\mathbf{k} \sqrt{k^2 + M_i^{*2}} (f_i(k) + \bar{f}_i(k)) + \frac{1}{2} m_\sigma^2 \sigma^2 + \frac{b}{3} (g_\sigma \sigma)^3 + \frac{c}{4} (g_\sigma \sigma)^4 + \frac{1}{2} m_\delta^2 \delta^2 + \frac{1}{2} m_\omega^2 \omega^2 + \frac{1}{2} m_\rho^2 \rho^2, \quad (5)$$

$$P^H = \sum_{i=p,n} \frac{1}{3} \frac{2}{(2\pi)^3} \int d^3\mathbf{k} \frac{k^2}{\sqrt{k^2 + M_i^{*2}}} (f_i(k) + \bar{f}_i(k)) - \frac{1}{2} m_\sigma^2 \sigma^2 - \frac{b}{3} (g_\sigma \sigma)^3 - \frac{c}{4} (g_\sigma \sigma)^4 - \frac{1}{2} m_\delta^2 \delta^2 + \frac{1}{2} m_\omega^2 \omega^2 + \frac{1}{2} m_\rho^2 \rho^2. \quad (6)$$

where  $f_i(k)$  and  $\bar{f}_i(k)$  are the fermion and antifermion distribution functions for proton and neutron ( $i = p, n$ ):

$$f_i(k) = \frac{1}{1 + \exp\{(E_i^*(k) - \mu_i^*)/T\}}, \quad (7)$$

$$\bar{f}_i(k) = \frac{1}{1 + \exp\{(E_i^*(k) + \mu_i^*)/T\}}. \quad (8)$$

The effective chemical potentials  $\mu_i^*$  are determined by the nucleon densities

$$\rho_i = 2 \int \frac{d^3\mathbf{k}}{(2\pi)^3} (f_i(k) - \bar{f}_i(k)). \quad (9)$$

With the baryon number density  $\rho = \rho_B^H = \rho_p + \rho_n$  and isospin density  $\rho_3^H = \rho_p - \rho_n$ . The asymmetry parameter can be defined as

$$\alpha^H \equiv -\frac{\rho_3^H}{\rho_B^H} = \frac{\rho_n - \rho_p}{\rho_p + \rho_n}. \quad (10)$$

In this study the parameter set  $NL\rho\delta$  [46] will be used to describe the properties of hadron matter. The model parameters is determined by calibrating the properties of symmetric nuclear matter at zero temperature and normal nuclear density. Our parameterizations are also tuned to reproduce collective flows and particle production at higher energies, where some hot and dense matter is probed, see [52] and refs. therein.

We take the PNJL model to describe the quark matter. In the pure gauge theory, the Polyakov-Loop serves as an order parameter for the  $\mathbb{Z}_3$  symmetry breaking transition from low to high temperature, i.e. for the transition from a confined to a deconfined phase. In the real world quarks are coupled to the Polyakov-Loop, which explicitly breaks the  $\mathbb{Z}_3$  symmetry. No rigorous order parameter is established for the deconfinement phase transition.

The energy density and pressure of nuclear matter at finite temperature are derived as

However, the Polyakov loop can still be practicable to distinguish a confined phase from a deconfined one.

The Lagrangian density in the three-flavor PNJL model is taken as

$$\begin{aligned} \mathcal{L}_q = & \bar{q}(i\gamma^\mu D_\mu - \hat{m}_0)q + G \sum_{k=0}^8 \left[ (\bar{q}\lambda_k q)^2 + (\bar{q}i\gamma_5 \lambda_k q)^2 \right] \\ & - K \left[ \det_f(\bar{q}(1 + \gamma_5)q) + \det_f(\bar{q}(1 - \gamma_5)q) \right] \\ & - \mathcal{U}(\Phi[A], \bar{\Phi}[A], T), \end{aligned} \quad (11)$$

where  $q$  denotes the quark fields with three flavors,  $u$ ,  $d$ , and  $s$ , and three colors;  $\hat{m}_0 = \text{diag}(m_u, m_d, m_s)$  in flavor space;  $G$  and  $K$  are the four-point and six-point interacting constants, respectively. The four-point interaction term in the Lagrangian keeps the  $SU_V(3) \times SU_A(3) \times U_V(1) \times U_A(1)$  symmetry, while the 't Hooft six-point interaction term breaks the  $U_A(1)$  symmetry.

The covariant derivative in the Lagrangian density is defined as  $D_\mu = \partial_\mu - iA_\mu$ . The gluon background field  $A_\mu = \delta_\mu^0 A_0$  is supposed to be homogeneous and static, with  $A_0 = g\mathcal{A}_0^a \frac{\lambda^a}{2}$ , where  $\frac{\lambda^a}{2}$  are  $SU(3)$  color generators. The effective potential  $\mathcal{U}(\Phi[A], \bar{\Phi}[A], T)$  is expressed in terms of the traced Polyakov loop  $\Phi = (\text{Tr}_c L)/N_C$  and its conjugate  $\bar{\Phi} = (\text{Tr}_c L^\dagger)/N_C$ . The Polyakov loop  $L$  is a matrix in color space

$$L(\vec{x}) = \mathcal{P} \exp \left[ i \int_0^\beta d\tau A_4(\vec{x}, \tau) \right], \quad (12)$$

where  $\beta = 1/T$  is the inverse of temperature and  $A_4 = iA_0$ .

The Polyakov loop can be expressed in a more intuitive physical form as

$$\Phi = \exp[-\beta F_q(\vec{x})] \quad (13)$$

where  $F_q$  is the free energy required to add an isolated quark to the system. So it will go from zero in the confined phase up to a finite value when deconfinement is reached [53].

Different effective potentials are adopted in the literature [30, 54, 55]. The logarithmic one given in [54] will be used in our calculation, which can reproduce well the data obtained in lattice calculation. The corresponding effective potential reads

$$\frac{\mathcal{U}(\Phi, \bar{\Phi}, T)}{T^4} = -\frac{a(T)}{2}\bar{\Phi}\Phi \quad (14)$$

$$+b(T)\ln\left[1 - 6\bar{\Phi}\Phi + 4(\bar{\Phi}^3 + \Phi^3) - 3(\bar{\Phi}\Phi)^2\right],$$

where

$$a(T) = a_0 + a_1\left(\frac{T_0}{T}\right) + a_2\left(\frac{T_0}{T}\right)^2, \quad (15)$$

and

$$b(T) = b_3\left(\frac{T_0}{T}\right)^3. \quad (16)$$

We note that in this version of PNJL the direct coupling between quark condensates and Polyakov loop is only via the covariant derivative in the Lagrangian density Eq.(11).

The parameters  $a_i$ ,  $b_i$  are precisely fitted according to the lattice result of QCD thermodynamics in pure

gauge sector.  $T_0$  is found to be 270 MeV as the critical temperature for the deconfinement phase transition of the gluon part at zero chemical potential [56]. When fermion fields are included, a rescaling of  $T_0$  is usually implemented to obtain consistent result between model calculation and full lattice simulation which gives a critical phase-transition temperature  $T_c = 173 \pm 8$  MeV [1, 2, 4]. In this study we rescale  $T_0 = 210$  MeV so as to produce  $T_c = 171$  MeV for the phase transition temperature at zero chemical potential.

In the mean field approximation, quarks can be seen as free quasiparticles with constituent masses  $M_i$ , and the dynamical quark masses (gap equations) are obtained as

$$M_i = m_i - 4G\phi_i + 2K\phi_j\phi_k \quad (i \neq j \neq k), \quad (17)$$

with  $i = u, d, s$ , where  $\phi_i$  stands for the quark condensate. The thermodynamic potential of the PNJL model at the mean field level is expressed as

$$\Omega = \mathcal{U}(\bar{\Phi}, \Phi, T) + 2G(\phi_u^2 + \phi_d^2 + \phi_s^2) - 4K\phi_u\phi_d\phi_s$$

$$-T \sum_n \int \frac{d^3p}{(2\pi)^3} \text{Tr} \ln \frac{S_i^{-1}(i\omega_n, \vec{p})}{T}. \quad (18)$$

Here  $S_i^{-1}(p) = -(p\!\!\!/ - M_i + \gamma_0(\mu_i - iA_4))$ , with  $\mu_i$  quark chemical potential, is the inverse fermion propagator in the background field  $A_4$ , and the trace has to be taken in color, flavor, and Dirac space. After summing over the fermion Matsubara frequencies,  $p^0 = i\omega_n = (2n+1)\pi T$ , the thermodynamic potential can be written as

$$\Omega = \mathcal{U}(\bar{\Phi}, \Phi, T) + 2G(\phi_u^2 + \phi_d^2 + \phi_s^2) - 4K\phi_u\phi_d\phi_s - 2 \int_{\Lambda} \frac{d^3p}{(2\pi)^3} 3(E_u + E_d + E_s)$$

$$-2T \sum_{u,d,s} \int \frac{d^3p}{(2\pi)^3} \left[ \ln(1 + 3\Phi e^{-(E_i - \mu_i)/T} + 3\bar{\Phi} e^{-2(E_i - \mu_i)/T} + e^{-3(E_i - \mu_i)/T}) \right]$$

$$-2T \sum_{u,d,s} \int \frac{d^3p}{(2\pi)^3} \left[ \ln(1 + 3\bar{\Phi} e^{-(E_i + \mu_i)/T} + 3\Phi e^{-2(E_i + \mu_i)/T} + e^{-3(E_i + \mu_i)/T}) \right], \quad (19)$$

where  $E_i = \sqrt{\vec{p}^2 + M_i^2}$  is the energy of quark flavor  $i$ .

We remark some interesting differences with respect to the thermodynamical potential derived within the pure NJL model, see [24, 50]. Apart the presence of the effective potential  $\mathcal{U}(\bar{\Phi}, \Phi, T)$ , the Polyakov loop is mostly acting on the quark-antiquark distribution functions, in the direction of a reduction, on the way to confinement. This is largely modifying the quark pressure, as seen in the calculations. Moreover, in spite of the minimal coupling introduced in the Lagrangian Eq.(11), only in the covariant derivative, the quark condensates will be strongly affected by the Polyakov loop via the modified  $q$ ,  $\bar{q}$  distribution functions. This will be also clearly observed in

the comparison of NJL and PNJL phase diagrams.

The values of  $\phi_u, \phi_d, \phi_s, \Phi$  and  $\bar{\Phi}$  are determined by minimizing the thermodynamical potential

$$\frac{\partial \Omega}{\partial \phi_u} = \frac{\partial \Omega}{\partial \phi_d} = \frac{\partial \Omega}{\partial \phi_s} = \frac{\partial \Omega}{\partial \Phi} = \frac{\partial \Omega}{\partial \bar{\Phi}} = 0. \quad (20)$$

All the thermodynamic quantities relevant to the bulk properties of quark matter can be obtained from  $\Omega$ . Especially, the pressure and energy density should be zero in the vacuum.

The baryon (isospin) density and baryon (isospin) chem-

ical potential in quark phase are defined as follows

$$\rho_B^Q = \frac{1}{3}(\rho_u + \rho_d), \quad \rho_3^Q = \rho_u - \rho_d, \quad (21)$$

and

$$\mu_B^Q = \frac{3}{2}(\mu_u + \mu_d), \quad \mu_3^Q = \frac{1}{2}(\mu_u - \mu_d). \quad (22)$$

The corresponding asymmetry parameter of quark phase is defined as

$$\alpha^Q \equiv -\frac{\rho_3^Q}{\rho_B^Q} = 3\frac{\rho_d - \rho_u}{\rho_u + \rho_d}. \quad (23)$$

As an effective model, the (P)NJL model is not renormalizable, so a cut-off  $\Lambda$  is implemented in 3-momentum space for divergent integrations. We take the model parameters:  $\Lambda = 603.2$  MeV,  $G\Lambda^2 = 1.835$ ,  $K\Lambda^5 = 12.36$ ,  $m_{u,d} = 5.5$  and  $m_s = 140.7$  MeV, determined by fitting  $f_\pi$ ,  $M_\pi$ ,  $m_K$  and  $m_\eta$  to their experimental values [25]. The coefficients in Polyakov effective potential are listed in Table I.

TABLE I: Parameters in Polyakov effective potential given in [54]

$a_0$	$a_1$	$a_2$	$a_3$
3.51	-2.47	15.2	-1.75

So far we have introduced how to describe the hadronic and quark phase by the RMF hadron model and PNJL quark model, respectively. The key point in the Two-EoS model is to construct the phase transition from hadronic to quark matter. As mentioned above, the two phases are connected by Gibbs criteria, i.e., the thermal, chemical and mechanical equilibrations being required. For the Hadron–quark–gluon phase transition relevant to heavy-ion collision of duration about  $10^{-22} \text{ sec}$ , ( $10 - 20 \text{ fm}/c$ ), thermal equilibration is only possible for strongly interacting processes, where baryon number and isospin conservations are preserved. So the strange-antistrange quark number may be rich, but the net strange quark number should be zero before the beginning of hadronization in the expansion stage [57], which can be approximately realized by requiring  $\mu_s = 0$  (Hadronization is out of the range of this study).

Based on the conservations of baryon number and isospin during strong interaction, the Gibbs conditions describing the phase transition can be expressed by

$$\begin{aligned} \mu_B^H(\rho_B, \rho_3, T) &= \mu_B^Q(\rho_B, \rho_3, T) \\ \mu_3^H(\rho_B, \rho_3, T) &= \mu_3^Q(\rho_B, \rho_3, T) \\ P^H(\rho_B, \rho_3, T) &= P^Q(\rho_B, \rho_3, T), \end{aligned} \quad (24)$$

where  $\rho_B = (1 - \chi)\rho_B^H + \chi\rho_B^Q$  and  $\rho_3 = (1 - \chi)\rho_3^H + \chi\rho_3^Q$  are the total baryon density, isospin density of the mixed

phase, respectively, and  $\chi$  is the fraction of quark matter. The global asymmetry parameter  $\alpha$  for the mixed phase is

$$\alpha \equiv -\frac{\rho_3}{\rho_B} = \frac{(1 - \chi)\rho_3^H + \chi\rho_3^Q}{(1 - \chi)\rho_B^H + \chi\rho_B^Q} = \alpha^H |_{\chi=0} = \alpha^Q |_{\chi=1}, \quad (25)$$

which is determined by the heavy-ion source formed in experiments.

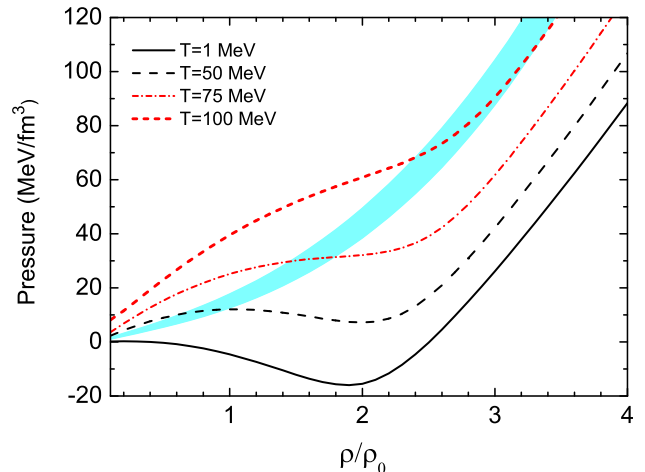


FIG. 1: Pressure of quark matter as function of baryon density at different temperatures in the NJL model. Isospin symmetric matter. In the shaded area we show also the Hadron (NL) curves in the temperature region between 75 and 100 MeV.

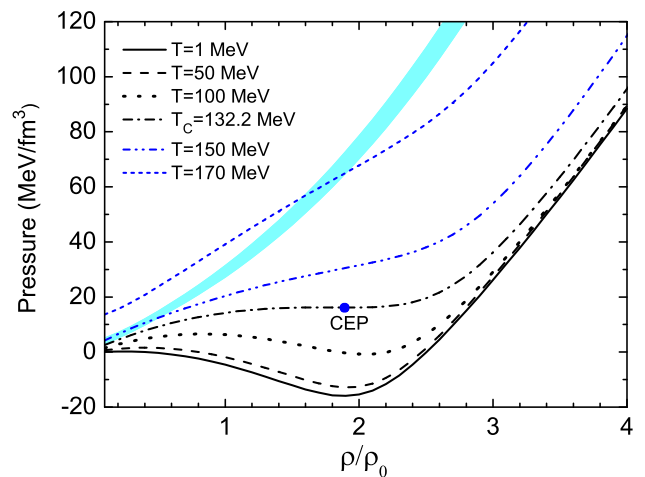


FIG. 2: Pressure of quark matter as function of baryon density at different temperatures in the PNJL model. Isospin symmetric matter. In the shaded area we show also the Hadron (NL) curves in the temperature region between 150 and 170 MeV.

### III. EXPECTED EFFECT OF THE CONFINEMENT DYNAMICS

Before showing detailed phase diagram results within the Two-EoS approach it is very instructive to analyze the effects of chiral and (de)confinement dynamics in the pure quark sector. In order to understand the physics which is behind we will show separately the results in the NJL, with the same parameters given before, and the PNJL model, for isospin symmetric matter. In Figs. 1, 2 we plot the pressure of isospin symmetric quark matter as function of baryon density for different temperatures respectively for the NJL and PNJL models. In this calculation isospin symmetric matter with  $\mu = \mu_u = \mu_d$  and  $\mu_s = 0$  is considered and  $\phi_l$  stands for the chiral condensate of  $u, d$  quarks.

From the two figures, we can see that the pressure has a local maximum and a local minimum at low temperature. The local extrema will disappear with the increase of temperature. The temperature with the disappearance of the two local extrema corresponds to the Critical-End-Point *CEP* of the first order chiral transition, for a more detailed discussion please refer to [24, 31]. It is interesting to note that the critical temperature of the chiral transition is rather different in the two cases, around 70 MeV in the NJL and around 130 MeV in the PNJL, while the density region is not much affected. This is due to the fact that for a fixed baryon density (or chemical potential) the NJL presents a much larger pressure for a given temperature, as clearly seen from the two figures 1, 2 [58]. This is a nice indication that when we have a coupling to the deconfinement, even if in the minimal way included here, the quark pressure at finite temperatures is reduced since the quarks degrees of freedom start to decrease.

All that will imply important differences at higher temperatures since above the chiral restoration the quark pressure will rapidly increase reaching an end-point in the Two-EoS approach where the matching to the hadron pressure will not be possible. This will happen in different points of the  $(T, \mu)$ ,  $(T, \rho)$  planes for the Hadron-NJL [50] and the Hadron-PNJL, and higher temperatures will be requested in the PNJL case. In fact this can be also clearly seen from Figs. 1 and 2, of the NJL- and PNJL-pressures, where we plot also the corresponding curves of the hadronic EoS in the end-point regions (shaded area). The Gibbs (Maxwell) conditions have no solution with decreasing density (chemical potential) and increasing temperature if we encounter a crossing of the hadron and quark curves in the  $T - \rho_B$  ( $T - \mu_B$ ) plane, with the quark pressure becoming larger than the hadron one. We see that this is happening for  $T \simeq 75$  MeV and  $\rho/\rho_0 \simeq 1.8$  in the NJL case and for  $T \simeq 170$  MeV and  $\rho/\rho_0 \simeq 1.6$  in the PNJL quark picture. In conclusion, due to the noticeable quark pressure difference at finite temperatures, besides the Critical-End-Points, we expect in general rather different phase diagrams given by the Hadron-NJL and Hadron-PNJL models. This will be seen in the Section

V, Figs. 8 and 9.

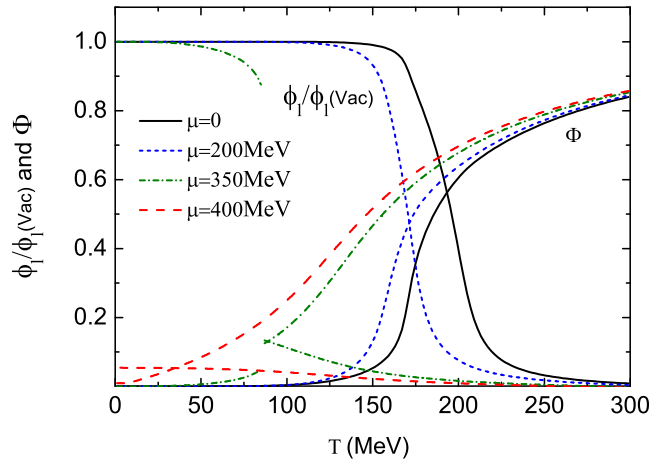


FIG. 3: Chiral condensate  $\phi_l$  (normalized to the vacuum value) and Polyakov-Loop  $\Phi$  as functions of temperature for various values of the quark chemical potential. Isospin symmetric matter.

### IV. PNJL PHASE DIAGRAM IN THE QUARK SECTOR

In order to better understand the effects of the coupling between quark condensates and Polyakov loop and also to compare with the Two-EoS results, we discuss here also the Phase diagram in the pure quark sector obtained from the PNJL model.

We plot in Fig. 3 the temperature evolution of the chiral condensate  $\phi_l$  and the Polyakov-Loop  $\Phi$  for various values of the quark chemical potential.  $\Phi$  and  $\bar{\Phi}$  have the same values at zero chemical potential and their difference is very small at finite chemical potential, hence we only present the results of  $\Phi$  in Fig. 3 and later in the discussion.

Firstly, we can see that the chiral condensate and Polyakov loop  $\Phi$  vary continuously at  $\mu = 0$  and 200 MeV, and there exist sharp decreases (increases) at high temperature indicating the onset of chiral (deconfinement) phase transitions. These characteristics show that the corresponding chiral and deconfinement phase transitions are crossovers for small chemical potential at high temperature. At variance, for large chemical potentials, e.g.,  $\mu = 350$  MeV, the chiral condensate varies discontinuously with the temperature, which indicates the presence of a first order chiral phase transition, as already seen in the pure NJL approach, although at much lower temperature [24], as discussed in the previous Section. The Polyakov loop is always showing a continuous behavior indicating that we have only crossover transitions. The jump observed for the dash-dotted curve corresponding to a  $\mu = 350$  MeV chemical potential is just an effect of the coupling to the sharp variation of the quark con-

densates at the first order chiral transition. Moreover this is happening in a region of very small values of the  $\Phi$  field at lower temperatures. As a matter of fact such discontinuity disappears for the results at  $\mu = 400$  MeV, i.e. above the chiral transition, see the dashed curves for both  $\phi$  and  $\Phi$  fields.

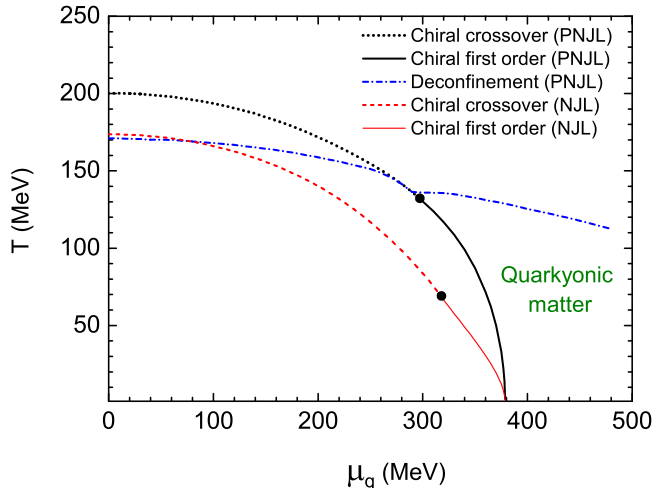


FIG. 4: Phase diagram of the PNJL model. The corresponding chiral phase transition for the pure NJL model is also shown. Isospin symmetric matter.

Finally in Fig. 4 we plot the phase diagram of the PNJL model in  $T - \mu_q$  plane (always for isospin symmetric matter). The phase transition curves are obtained by requiring  $\partial\phi_i/\partial T$  and  $\partial\Phi/\partial T$  taking the maximum values. For deconfinement phase transition the use of the maximum value of  $\partial\Phi/\partial T$  as the phase-transition tracer is a good choice when  $\mu$  is not too large. In fact we see from Fig. 3 a sharp increase of  $\Phi$  for  $\mu = 0$  and 200 MeV. However, with the increase of chemical potential, although we are still able to observe the maximum of  $\partial\Phi/\partial T$ , the width of the maximum increases. The peaks of  $\partial\Phi/\partial T$  are more smoothed and this will be not any more a well defined phase-transition parameter as  $\mu$  is large. Therefore, some authors take  $\Phi = 1/2$  as the phase transition parameter [55, 59, 60]. In conclusion from Fig. 3 we can see that the chiral phase transition is continuous at high temperature and relatively smaller chemical potential, while a first order phase transition takes place at low temperature and larger chemical potential. The *Critical-End-Point* (*CEP*) of the chiral transition appears at (132.2, 296.6) MeV in the  $T - \mu_q$  plane, in agreement with similar calculations [60]. At variance, the deconfinement phase transition is always a continuous crossover in the PNJL model, but the peak of  $\partial\Phi/\partial T$  becomes more and more smooth with the increase of baryon chemical potential. In addition, at large chemical potential, a chirally restored but still confined matter, the *quarkyonic matter*, can be realized in the PNJL model. All that is reported in Fig. 4 where we plot the full phase

diagram of the PNJL approach.

Here we give a short discussion about the coincidence of chiral and deconfinement phase transitions as well as the presence of quarkyonic matter. The temperature dependence of the chiral condensate and of the Polyakov loop of Fig. 3 as well the PNJL phase diagram of Fig. 4 are obtained with the rescaled parameter  $T_0 = 210$  MeV. The coincidence of chiral restoration and deconfinement takes place at about  $\mu_q = 290$  MeV. If we take  $T_0 = 270$  MeV, the approximate coincidence, with the different phase-transition temperatures less than 10 MeV, will move down to  $\mu \simeq 0$ . In any case, there is only one cross point of the two phase transitions. Up to now, the relation between chiral-symmetry restoration and deconfinement phase transition is still an open question. It is possible that the coincidence of chiral and deconfinement phase transition takes place in a wider range of chemical potentials. Such coincidence indeed has been recently realized by considering a larger coupling (*entanglement*) between chiral condensate and Polyakov loop, with an explicit  $\Phi$ -dependence of the condensate coupling  $G(\Phi)$  and a chemical potential dependent  $T_0$  [59, 60].

In the same Fig. 4 we report also the chiral transition curve for the pure NJL model (same parameters). We note the coupling between the chiral condensates and the Polyakov-Loop fields ( $\Phi$ ,  $\bar{\Phi}$ ) is mostly affecting the temperature of the chiral *CEP* as expected from the pressure discussion of the previous Section.

From Fig. 4 we can see that the deconfinement phase-transition temperature is still high at large chemical potential, and so the region of quarkyonic matter appears very wide. On the other hand the signature of a deconfinement transition is disappearing at large chemical potentials and lower temperatures. Because of the lack of lattice QCD data at large real chemical potentials, more investigations are needed to study the physics in this range. The results in [59] also show that the range of quarkyonic matter shrinks when a  $\mu$ -dependent  $T_0$  and/or a larger entanglement between quark condensate and Polyakov loop is considered.

We remark that this  $(T - \mu)$  zone just represents the nuclear matter phase diagram region possibly reached in the collision of heavy ions at intermediate energies and so it is of large interest to perform Two-EoS predictions, which should have a good connection to the more fundamental results of effective quark models. This is the subject of the next Section.

## V. HADRON-QUARK PHASE TRANSITIONS

In the following we will discuss the phase diagrams obtained in the Two-EoS model, i.e., explicitly considering a hadronic EoS with the parameter set of  $NL$  for symmetric matter and  $NL\rho\delta$  for asymmetric matter at low density and chemical potential [45, 46].

We present firstly the phase transition from hadronic

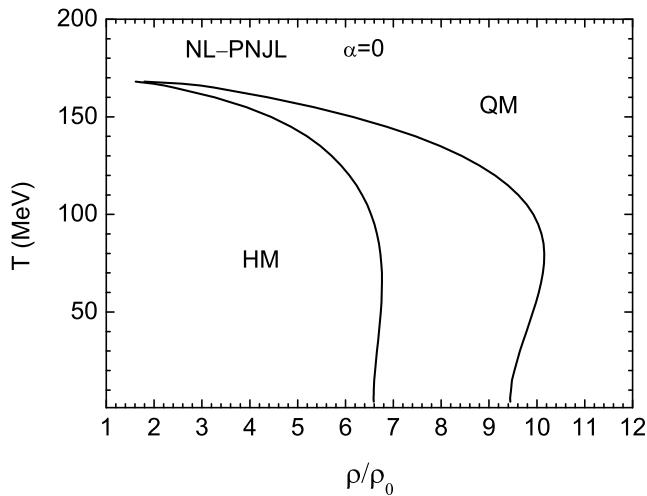


FIG. 5: Phase diagram in  $T - \rho_B$  plane in the Two-EoS model for symmetric matter.

to deconfined quark phase in  $T - \rho_B$  plane in Fig. 5 for symmetric matter and in Fig. 6 for asymmetric matter with the global asymmetry parameter  $\alpha = 0.2$ .

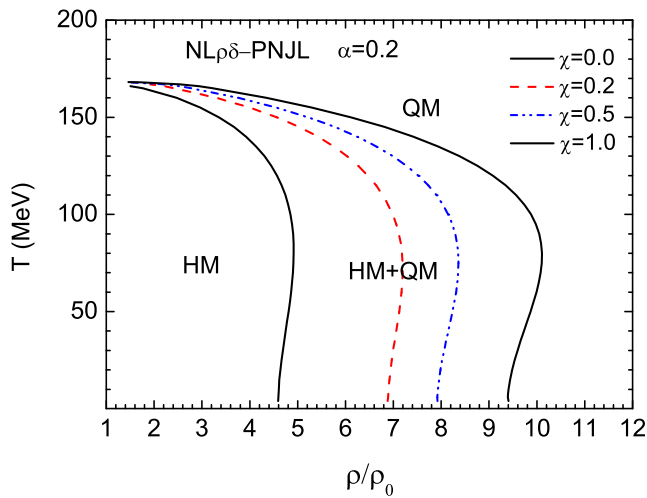


FIG. 6: Phase diagram in  $T - \rho_B$  plane in the Two-EoS model for asymmetric matter with the global asymmetry parameter  $\alpha = 0.2$ .  $\chi$  represents the fraction of quark matter.

For symmetric matter at a fixed  $T$ , the first order phase transition takes place with the same pressure and  $\mu_B$  in both phases, but a jump of  $\rho_B^H$  to  $\rho_B^Q$ , just as shown in Fig. 5. In the mixed phase, the pressures of both phases keep unchanged and  $\alpha = \alpha^H = \alpha^Q = 0$  for any quark fraction  $\chi$ . These features are quite different for the mixed phase in isospin asymmetric matter. As already noted in [50], where the NJL quark EoS has been used, also in the PNJL case we see a clear Isospin Distillation effect, i.e., a strong enhancement of the isospin asymme-

try in the quark component inside the mixed phase, as reported in Fig. 7, where the asymmetry parameter in the two components are plotted vs. the quark fraction  $\chi$ . As a consequence the pressure in the mixed phase keeps rising with  $\chi$ , more rapidly for quark concentrations below 50% [50].

From Fig. 7 we remark that this isospin enrichment of the quark phase is rather robust vs. the increasing temperature. This is important since color pairing correlations at low temperatures will decrease symmetry energy effects [49]. We have to note that such large isospin distillation effect is due to the large difference in the symmetry terms in the two phases, mainly because all the used quark effective models do not have explicit isovector fields in the interaction [47].

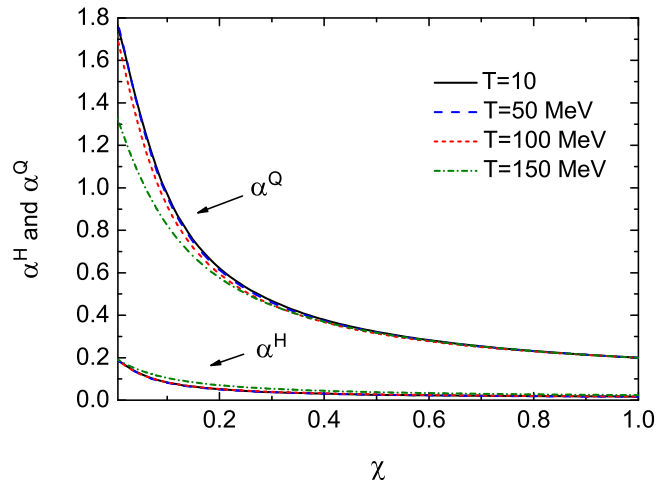


FIG. 7: The behavior of local asymmetric parameters  $\alpha^H$  and  $\alpha^Q$  in the mixed phase for several values of temperature. Parameter set  $NL\rho\delta$  is used in the calculation.

Such behavior of the local asymmetry parameters will possibly produce some observational signals in the following hadronization during the expansion. We can expect an inverse trend in the emission of neutron rich clusters, as well as an enhancement of  $\pi^-/\pi^+$ ,  $K^0/K^+$  yield ratios from the high density n-rich regions which undergo the transition. Besides, an enhancement of the production of isospin-rich resonances and subsequent decays may be found. For more details one can refer to [47, 50]. Moreover, an evident feature of Fig. 6 is that the onset density of hadron-quark phase transition for asymmetric matter is much lower than that of the symmetric one, and therefore it will be easier to probe in heavy-ion collision experiments.

We plot the  $T - \mu_B$  phase diagrams in Fig. 8 for symmetric matter and Fig. 9 for asymmetric matter. Fig. 8 clearly shows that there is only one phase-transition curve in the  $T - \mu_B$  plane. The phase transition curve is independent of the quark fraction  $\chi$ . However, for asymmetric matter, the phase transition curve varies for different quark fraction  $\chi$ . The phase transition curves



in Fig. 9 are obtained with  $\chi = 0$  and 1, representing the beginning and the end of hadron-quark phase transition, respectively.

In Fig. 8 and Fig. 9 we also plot the phase transition curves with the Hadron-NJL model. For the NJL model with only chiral dynamics, no physical solution exists when the temperature is higher than  $\sim 80$  MeV. The corresponding temperature is enhanced to about  $\sim 166$  MeV with the Hadron-PNJL model, which is closer to the phase transition (crossover) temperature given by full lattice calculation at zero or small chemical potential [1, 2, 4]. In this sense the Hadron-PNJL model gives significantly different results and represents certainly an improvement respect to the Hadron-NJL scheme of ref. [50]. From Fig. 9 we remark that in both cases the region around the *Critical – End – Points* is not affected by isospin asymmetry contributions, which are relevant at lower temperatures and larger chemical potentials.

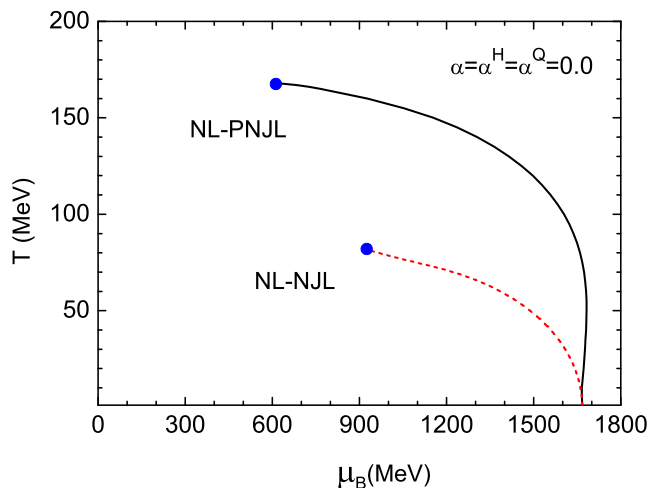


FIG. 8: Phase diagram in  $T - \mu_B$  plane for symmetric matter.

From the detailed discussions of the previous two Sections now we nicely understand the large difference between Hadron-NJL and Hadron-PNJL phase transitions and the important role of the confinement dynamics.

Finally in Fig. 10 we present together the phase diagrams obtained by the PNJL model and the Hadron-PNJL model. We find that the deconfined phase transition curve in the PNJL model is close to that obtained in the Hadron-PNJL model at high temperature and intermediate chemical potential. At larger chemical potential, the deconfinement phase transition curve in the PNJL model has still a high temperature. On the other hand from the previous Section we have seen that deconfinement phase transition order parameter  $\Phi$  cannot describe well the phase transition at larger chemical potential and lower temperatures. We must rely on the predictions of the Two-EoS approach, which in fact nicely show a good connection to the results more reliable of the PNJL quark model, at high temperature and small or vanishing chem-

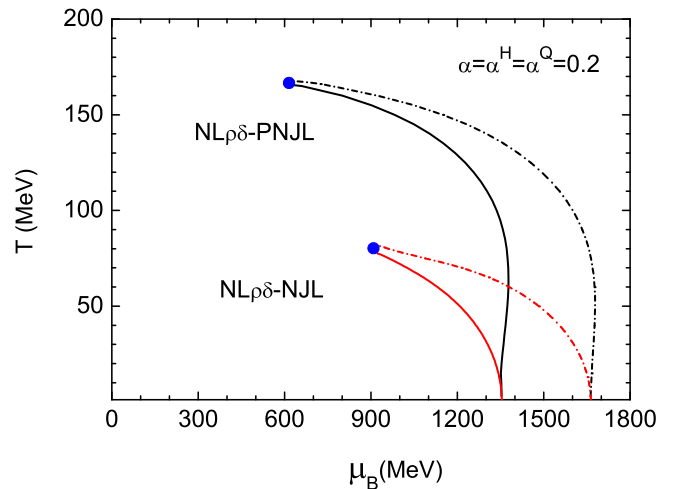


FIG. 9: Phase diagram in  $T - \mu_B$  plane for asymmetric matter with the global asymmetry parameter  $\alpha = 0.2$ .

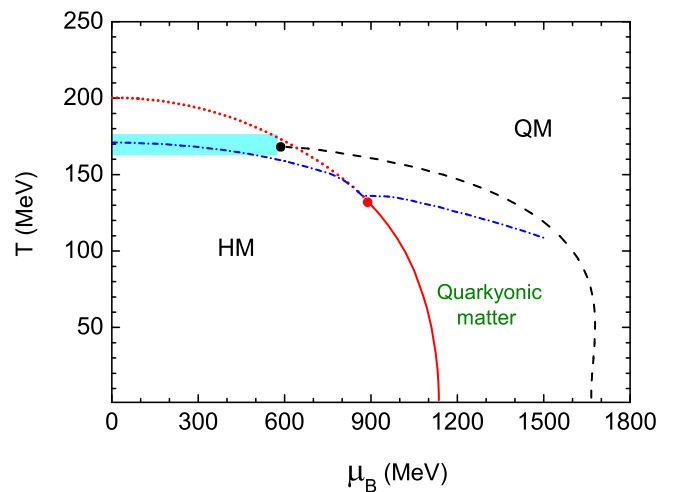


FIG. 10: Phase diagrams of the PNJL model and the Two-EoS model (dashed curve). The shaded area is just a guide for the eye.

ical potential. The Two-EoS Hadron-(P)NJL model also shows that the phase transition at low temperature takes place at much larger chemical potential, consistent with the expectation of a more relevant contribution from the hadron sector [51].

We notice that at  $T = 0$  there is no difference between the Hadron-NJL and Hadron-PNJL models. This is due to the fact that there is no dependence of  $\Phi$  on  $\mu_B$ , therefore it vanishes and the PNJL reduces to the NJL. This may casts some doubts on the reliability of the present calculations at  $T = 0$  and large  $\mu_B$ . However our main interest is a region at finite  $T$  ( $T \simeq 50 - 100$  MeV) and  $\mu_B$  ( $\mu_B \simeq 1000 - 2000$  MeV) region that can be reached by Heavy Ion Collisions at relativistic energies.

Moreover the results obtained by the Hadron-PNJL

model at high  $T$ , small  $\mu_B$  and low  $T$ , large  $\mu_B$  may be improved with the consideration of a stronger entanglement between chiral condensate and Polyakov loop, and a chemical potential dependent  $T_0$  [59, 60]. The relevant investigation will be performed as a further study. In any case, since we lack of reliable lattice data at large chemical potential, in general more theoretical work is encouraged.

## VI. SUMMARY

In this study, the hadron-quark phase transition are investigated in the Two-EoS model. The nonlinear Walecka model and the PNJL(NJL) model are used to describe hadron matter and quark matter, separately. We follow the Gibbs criteria to construct the mixed phase with baryon number and isospin conservations, likely reached during the hot and dense phase formed in heavy-ion collision at intermediate energies. The parameters in both models are well fitted to give a good description of the properties of nuclear matter (even isospin asymmetric), at saturation as well as at higher baryon densities, or lattice data at high temperature with zero/small chemical potential.

The phase diagrams for both symmetric and asymmetric matter are explored in both  $T-\rho_B$  and  $T-\mu_B$  planes. In both Hadron-(P)NJL calculations we get a first order phase transition with a Critical-End-Point at finite temperature and chemical potential. In the PNJL case the *CEP* is shifted to larger temperatures and smaller chemical potential, to the (166, 600) MeV point in the  $(T, \mu_B)$  plane. This appears a nice indication of a decrease of the quark pressure when confinement is accounted for. Such result is particularly interesting since the *CEP* is now in the region of  $\mu_q/T_c \simeq 1$  (where  $\mu_q$  is the quark chemical potential) and so it could be reached with some confidence by lattice-QCD complete calculations.

Another interesting result is that isospin effects are almost negligible when we approach the *CEP*. At variance the calculation shows that the onset density of asymmetric matter is lower than that of symmetric matter. Moreover in the mixed phase of asymmetric matter, the decreasing of local asymmetry parameter  $\alpha^H$  and  $\alpha^Q$  with the increasing quark fraction  $\chi$  may produce some observable signals. In particular we remark the noticeable isospin distillation mechanism (isospin enrichment of the quark phase) at the beginning of the mixed phase, i.e. for low quark fractions, that should show up in the hadronization stage during the expansion. We also see from Fig.7 that this effect is still there even at relatively large temperatures, certainly present in the high density stage of heavy ion collisions at relativistic energies [46, 52]. All that support the possibility of an experimental observation in the new planned facilities, for example, FAIR at GSI-Darmstadt and NICA at JINR-Dubna, with realistic asymmetries for stable/unstable beams. Some expected possible signals are suggested.

Because of the lack of lattice data at larger real chemical potential, we are left with the puzzle between chiral symmetry restoration and deconfinement. More investigations on the chiral dynamics and (de)confinement, as well as their entanglement are needed. The improvement of the understanding of quark-matter interaction is beneficial to get more accurate results in the Two-EoS model.

## Acknowledgments

This project has been supported in part by the National Natural Science Foundation of China under Grants Nos. 10875160, 11075037, 10935001 and the Major State Basic Research Development Program under Contract No. G2007CB815000. This work has been partially performed under the FIRB Research Grant RBFR0814TT provided by the MIUR.

- 
- [1] F. Karsch, E. Laermann, and A. Peikert, Nucl. Phys. B **605**, 579 (2001).
  - [2] F. Karsch, Nucl. Phys. A **698**, 199 (2002).
  - [3] C. R. Allton et al., Phys. Rev. D **66**, 074507 (2002).
  - [4] M. Kaczmarek and F. Zantow, Phys. Rev. D **71**, 114510 (2005).
  - [5] M. Cheng et al., Phys. Rev. D **74**, 054507 (2006).
  - [6] Y. Aoki, et al., JHEP **06**, 088 (2009).
  - [7] S. Borsányi et al., JHEP **09**, 073 (2010).
  - [8] Z. Fodor and S.D. Katz, Phys. Lett. B **534**, 87 (2002); JHEP **03**, 014 (2002).
  - [9] Z. Fodor, S.D. Katz, and C. Schmidt, JHEP **03**, 121 (2007).
  - [10] M. D'Elia and F. Sanfilippo, Phys. Rev. D **80**, 014502 (2009).
  - [11] S. Ejiri, Phys. Rev. D **78**, 074507 (2008).
  - [12] M. A. Clark and A. D. Kennedy, Phys. Rev. Lett. **98**, 051601 (2007).
  - [13] K. Fukushima and T. Hatsuda, Rep. Prog. Phys. **74**, 014001 (2011).
  - [14] Y. Nambu and G. Jona-Lasinio, Phys. Rev. **112**, 345 (1961); Phys. Rev. **124**, 246 (1961).
  - [15] D. Toublan and J. B. Kogut, Phys. Lett. B **564**, 212 (2003).
  - [16] S. B. Ruster, V. Werth, M. Buballa, I. A. Shovkovy, and D. H. Rischke, Phys. Rev. D **72**, 034004 (2005).
  - [17] H. Abuki, and T. Kunihiro, Nucl. Phys. A **768**, 118 (2006).
  - [18] Si-xue Qin, Lei Chang, Huan Chen, Yu-xin Liu, Craig D. Roberts, Phys. Rev. Lett. **106**, 172301 (2001).
  - [19] M. K. Volkov, Ann. Phys.(N.Y.) **157**, 282 (1984).
  - [20] T. Hatsuda and T. Kunihiro, Phys. Lett. B **145**, 7 (1984).
  - [21] S. P. Klevansky, Rev. Mod. Phys. **64**, 649 (1992).
  - [22] T. Hatsuda and T. Kunihiro, Phys. Rep. **247**, 221 (1994).
  - [23] R. Alkofer, H. Reinhardt, and H. Weigel, Phys. Rep. **265**, 239 (1996).

- [24] M. Buballa, Phys. Rep. **407**, 205 (2005).
- [25] P. Rehberg, S. P. Klevansky, and J. Hüfner, Phys. Rev. C **53**, 410 (1995).
- [26] I. Shovkovy, and Mei Huang, Nucl. Phys. B **564**, 205 (2003).
- [27] M. Huang and I. Shovkovy, Nucl. Phys. A **729**, 835 (2003).
- [28] M. Alford, A. Schmit, K. Rajagopal, and T. Schäfer, Rev. Mod. Phys. **80**, 1455 (2008), and refs. therein.
- [29] K. Fukushima, Phys. Lett. B **591**, 277 (2004).
- [30] C. Ratti, M.A. Thaler, W. Weise, Phys. Rev. D **73**, 014019 (2006).
- [31] P. Costa, M. C. Ruivo, C. A. de Sousa, and H. Hansen, Symmetry **2**(3), 1338 (2010).
- [32] B.-J. Schaefer, M. Wagner, J. Wambach, Phys. Rev. D **81**, 074013 (2010).
- [33] T. K. Herbst, J. M. Pawłowski, B.-J. Schaefer, Phys. Lett. B **696**, 58 (2011).
- [34] K. Kashiwa, H. Kouno, M. Matsuzaki and M. Yahiro, Nucl. Phys. B **662**, 26 (2008).
- [35] H. Abuki, R. Anglani, R. Gatto, G. Nardulli and M. Ruggieri, Phys. Rev. D **78**, 034034 (2008).
- [36] W. J. Fu, Z. Zhang, Y. X. Liu, Phys. Rev. D **77**, 014006 (2008).
- [37] N. K. Glendenning, Phys. Rev. D **46**, 1274 (1992).
- [38] N. K. Glendenning and J. Schaffner-Bielich, Phys. Rev. Lett. **81**, 4564 (1998); Phys. Rev. C **60**, 025803 (1999).
- [39] G. F. Burgio, M. Baldo, P. K. Sahu, and H.-J. Schulze, Phys. Rev. C **66**, 025802 (2002).
- [40] T. Maruyama, S. Chiba, H.-J. Schulze, and T. Tatsumi, Phys. Rev. D **76**, 123015 (2007).
- [41] F. Yang and H. Shen, Phys. Rev. C **77**, 025801 (2008).
- [42] G. Y. Shao and Y. X. Liu, Phys. Rev. C **82**, 055801 (2010).
- [43] J. Xu, L. W. Chen, C. M Ko, and B. A. Li, Phys. Rev. C **81**, 055803 (2010).
- [44] H. Müller, Nucl. Phys. A **618**, 349 (1997).
- [45] V. Baran, M. Colonna, V. Greco, M. Di Toro, Phys. Rep. **410**, 335 (2005).
- [46] M. Di Toro, A. Drago, T. Gaitanos, V. Greco, and A. Lavagno, Nucl. Phys. A **775**, 102 (2006).
- [47] M. Di Toro *et al.*, Phys. Rev. C **83**, 014911 (2011).
- [48] R. Cavagnoli, C. Providência, and D. P. Menezes, Phys. Rev. C **83**, 045201 (2011).
- [49] G. Pagliara and J. Schaffner-Bielich, Phys. Rev. D **81**, 094024 (2010).
- [50] G. Y. Shao, M. Di Toro, B. Liu, M. Colonna, V. Greco, Y. X. Liu, S. Plumari, *Hadron-quark phase transition in asymmetric matter with dynamical quark masses*, arXiv:1102.4964, to appear in Phys. Rev. D (2011).
- [51] B. Liu, M. Di Toro, G. Y. Shao, V. Greco, C. W. Shen, Z. H. Li, *Phase transitions to quark matter at finite T and  $\mu_B$*  arXiv:1105.0555[nucl.th.]
- [52] M. Di Toro *et al.*, Prog. Part. Nucl. Phys. **62**, 389 (2009).
- [53] L.D. Mc Larren and B. Svetitski, Phys. Rev. D **24**, 450 (1981).
- [54] S. Röbner, C. Ratti, and W. Weise, Phys. Rev. D **75**, 034007 (2007).
- [55] K. Fukushima, Phys. Rev. D **77**, 114028 (2008).
- [56] M. Fukugita, M. Okawa, and A. Ukawa, Nucl. Phys. B **337**, 191 (1990).
- [57] C. Greiner, P. Koch, and H. Stoecker, Phys. Rev. Lett. **58**, 1825 (1987).
- [58] H. Hansen, W. M. Alberico, A. Beraudo, A. Molinari, M. Nardi, and C. Ratti, Phys. Rev. D **75**, 065004 (2007).
- [59] Y. Sakai, T. Sasaki, H. Kouno, and M. Yahiro, arXiv:1104.2394v1.
- [60] Y. Sakai, T. Sasaki, H. Kouno, and M. Yahiro, Phys. Rev. D **82**, 076003 (2010).